DOI 10.1007/s11182-019-01724-w

Russian Physics Journal, Vol. 62, No. 3, July, 2019 (Russian Original No. 3, March, 2019)

OPTICS AND SPECTROSCOPY

OPTICALLY INDUCED CHANNEL WAVEGUIDE STRUCTURES WITH SPATIAL MODULATION OF PARAMETERS IN THE SURFACE LAYER OF LITHIUM NIOBATE

A. D. Bezpaly, V. M. Shandarov, A. E. Mandel, V. I. Bykov, and K. M. Mambetova

UDC 535:621.372.8

Results of experimental studies of channel optical waveguide structures with spatially-modulated parameters obtained by point-by-point inducing of refractive index perturbations upon exposure to laser radiation of visible range in Y-cut $LiNbO_3$ *samples with photorefractive surface layer are presented.*

Keywords: channel waveguide, lithium niobate ($LiNbO_3$), photorefractive effect, spatial modulation, exposure, probing.

INTRODUCTION

Lithium niobate ($LiNbO_3$) single crystals are widely used for the development of various elements and devices of integral and nonlinear optics, photonics, and laser technology by virtue of a unique set of physical properties [1]. Doping of lithium niobate with ions of transitive metals, such as Fe, Cu, and Mn that can be in the crystal in several charge states considerably increases its photorefractive response [2]. The photorefractive effect consisting in perturbation of the refractive index of $LiNbO_3$ samples doped with such impurities upon exposure to light is caused by the photovoltaic mechanism of charge carrier transfer and does not require application of an external electric field to provide drift of these carriers. In $LiNbO_3$ crystals with photovoltaic nonlinear response, the optical properties also change upon exposure to light with low intensity of the order of 0.1 W/cm^2 and less. Phase diffraction gratings and more complex holographic structures can be formed in them upon exposure to radiation of low-power continuous lasers [3, 4]. This opens prospects for the development of hybrid optoelectronic and fully optical photonics devices [5, 6]. In photorefractive crystals, optical waveguide elements can be induced by spatial optical solitons [7]; however, the nonlinear response of the transport mechanism in $LiNbO_3$ is self-defocusing in character [8]. Hence, only dark spatial solitons can be formed in this crystal by this mechanism [8, 9].

Doping impurities can be incorporated into a charge during crystal growth or implanted through the optically polished surface of samples using diffusion, ionic exchange, and ionic implantation methods [5, 9, 10]. The change of the physical properties of the material near the surface can cause the occurrence in this region of the optical waveguide or laser properties [5, 9, 10] and also can modify its acoustic and optical parameters [5, 11]. Surface doping allows one to obtain higher concentrations of impurities in comparison with their incorporation during crystal growth. In this case, the required surface areas of the sample can be doped with different impurities or their combinations to change the functional designation of these areas [12].

Tomsk State University of Control Systems and Radioelectronics, Tomsk, Russia, e-mail: id_alex@list.ru; mandelae@svch.tusur.ru; vitalii.i.bykov@tusur.ru; mambetova_ksenia@mail.ru. Translated from Izvestiya Vysshikh Uchebnykh Zavedenii, Fizika, No. 3, pp. 3–8, March, 2019. Original article submitted October 16, 2018.

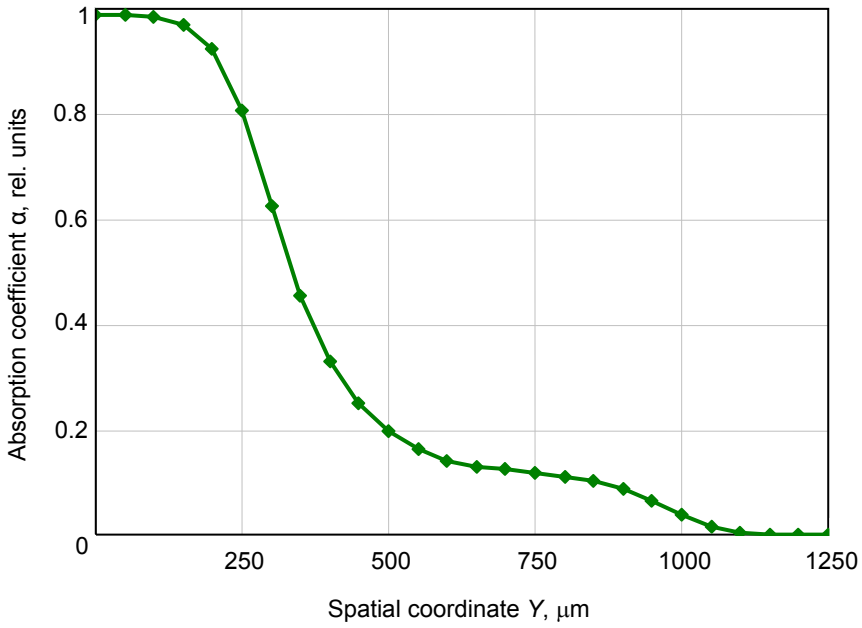

Fig. 1. Light absorption measured with radiation incident at the crystal end face.

The purpose of the present work is a study of optically induced channel optical waveguides in *Y*-cut lithium niobate crystal samples with surface Cu-ion doping using a spatially moving recording laser beam. The parameters of the formed waveguides are studied by the method of probing by light with the wavelength λ = 633 nm and polarization corresponding to that of the extraordinary wave in the crystal.

1. FORMATION OF CHANNEL WAVEGUIDE STRUCTURES

Experiments on the development of waveguide elements were performed with a *Y*-cut Cu:$LiNbO_3$ plate with sizes 30 × 3 × 15 mm along the *X*, *Y*, and *Z* axes, respectively. Copper ions were incorporated into the crystal using surface doping. For this purpose, Cu films ~200 nm thick were deposited on the *XZ* crystal surface by thermal sputtering in vacuum. Then the diffusion process in air proceeded at a temperature of 900°C during 10 h. As a result, a Cu:$LiNbO_3$ layer was formed in the subsurface region. The layer thickness was estimated by probing of the sample from the end face by radiation with λ = 532 nm and output power *P* = 2 mW. The light beam was focused onto the end face of the crystal using a spherical lens with the focal length *F* = 25 cm. The crystal was put on a linear translator with translation accuracy of 10 μm. The sample was displaced relative to incident radiation with 50 μm step size. The intensity of radiation transmitted through the crystal was recorded with a photodiode (PD). From the data obtained with the PD, the absorption coefficients in the crystal were calculated with a step size of 50 μm. As a result, the dependence of the laser radiation absorption in the sample was obtained shown in Fig. 1. The doped layer thickness estimated at a level of 0.95 of the maximum coefficient α was $h \approx 200$ μm.

Channel optical waveguides were formed at the expense of the photorefractive effect [13, 14] using the experimental setup whose block is shown in Fig. 2.

A light beam from radiation source *1* for which we used a solid-state YAG:Nd^{3+} laser with frequency doubling (λ = 532 nm) and output power of 10 mW was focused onto the *XZ* surface of Cu:$LiNbO_3$ sample *4* put on mobile table *3* with microobjective *2* having magnification ×10. The light intensity distribution over the surface was recorded with a BS-FW-FX33 laser beam analyzer (LBA) interfaced to a personal computer. The focused beam diameter in the waist region at the level 1/*e* of the maximum intensity was ~20 μm. Mobile table *3* represented a micrometric positioner and was used to set the sample position relative to the forming beam with accuracy of 5 μm.

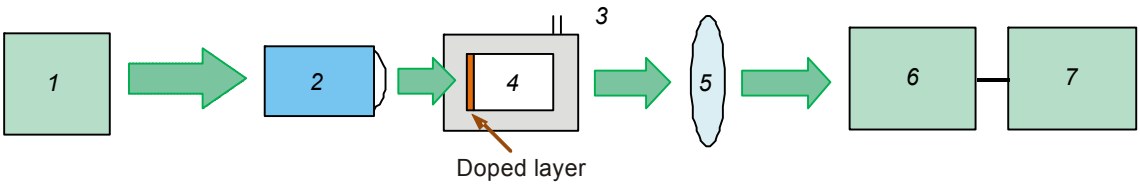

Fig. 2. Block diagram of the experimental setup for forming channel waveguide structures comprising radiation source *1*, microobjective *2*, micrometer table *3*, lithium niobate crystal *4*, imaging lens *5*, laser beam analyzer *6*, and personal computer *7*.

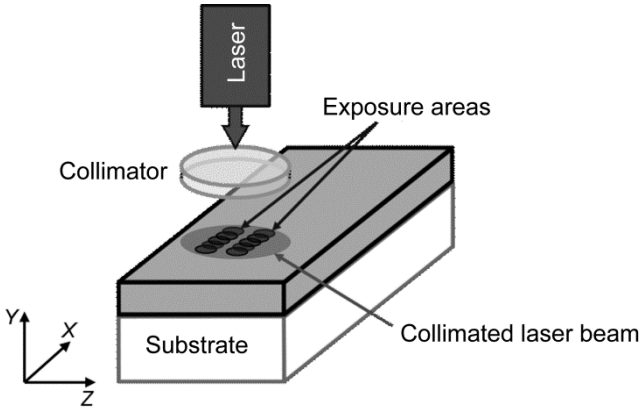

Fig. 3. Schematic image of probing of induced waveguide structures.

The point-by-point surface exposure with sample displacement step size 20–60 μm led to the formation in the subsurface Cu:$LiNbO_3$ doped layer of areas with reduced refractive index whose lengths varied from 1 to 2 mm. The orientation of the polarization vector of acting radiation along the *X* axis of the crystal corresponded to that of the ordinary wave. To obtain the waveguide effect, the structures were formed consisting of two parallel bands oriented along the *X* axis of the crystal [13].

2. INVESTIGATION OF THE INDUCED CHANNEL WAVEGUIDE STRUCTURES

For the photovoltaic mechanism of electron transfer in the conduction band, the $LiNbO_3$ refractive indices in the exposed areas decrease due to the photorefractive effect [3, 5]; therefore, the optical waveguide effect can be manifested between two neighboring areas. In our experiments, exposed areas represented parallel bands oriented in the direction of the *X* axis of the crystal. Each band was formed upon successive exposure of the $LiNbO_3$ surface to the focused light beam and comprised a set of points. The number of exposure points and the distance between their centers was varied in different experiments. The distance between the band centers in different experiments was 40–60 μm. The point exposure time in different experiments changed from 5 to 12 s. Inhomogeneities induced in the doped $LiNbO_3$ surface were probed by a He–Ne-laser collimated beam (λ = 633 nm) 1 mm in diameter (Fig. 3).

Some results of probing of the formed structures are shown in Fig. 4. Figure 4*a* shows the result of probing of the waveguide structure homogeneous in the longitudinal direction. Two parallel dark bands in the central part of the figure were formed by inducing spots with a distance between their centers of 20 μm. These bands show areas with refractive index reduced due to the photorefractive effect. A light band between them is the waveguide region.

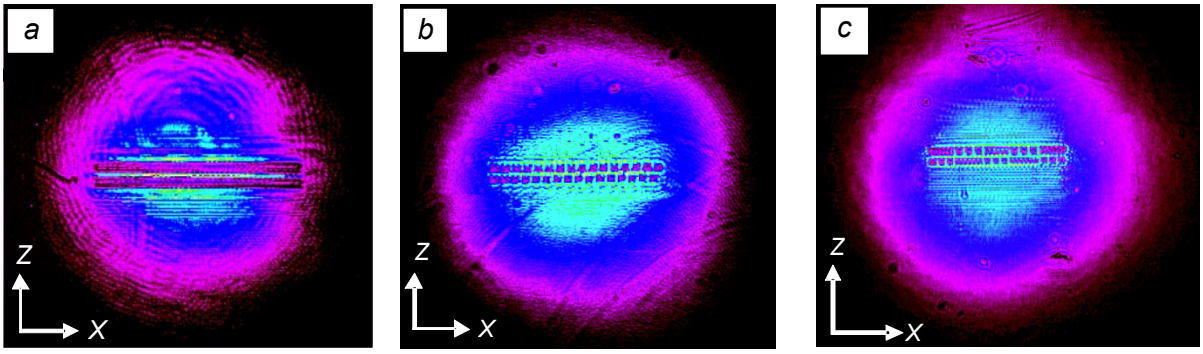

Fig. 4. Light images obtained by probing channel waveguide structures: *a*) longitudinally homogeneous, *b*) periodically inhomogeneous, and *c*) with variable degree of inhomogeneity.

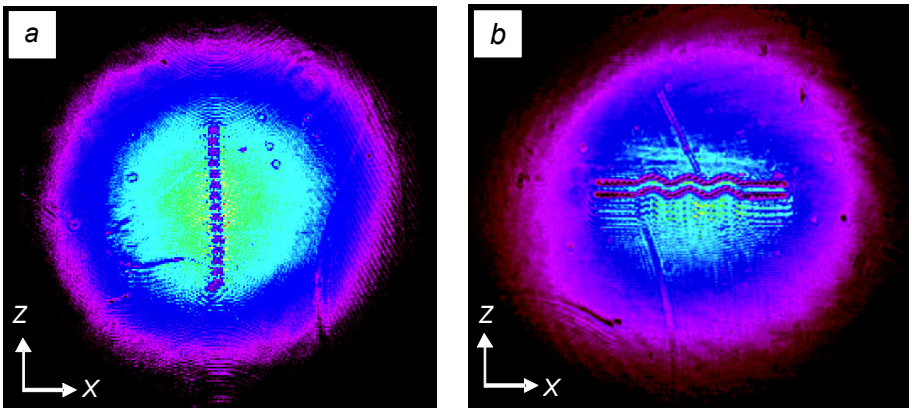

Fig. 5. Light images obtained by probing of *a*) exposure band oriented along the optical crystal axis and *b*) induced structure with complex topology.

Figure 4*b* shows the result of probing of the waveguide structure formed by inducing spots with a distance between their centers of 60 μm. This case corresponds to the waveguide channel structure with periodic inhomogeneity in the longitudinal direction. The width of the waveguide region for homogeneous and inhomogeneous structures is ~20 μm. An example of the waveguide structures with variable spatial modulation in the longitudinal direction is shown in Fig. 4*c*. In the process of forming the induced structures, the step between exposure spots varied from 20 to 50 μm.

Formation of the photorefractive phase elements is complicated when the exposure band was oriented along the optical axis of the crystal [5]. This is due to the fact that the spatial charge field arises only at the boundaries of the exposure area perpendicular to the direction of the optical crystal axis. However, the point-by-point exposure of the crystal surface to a narrow light beam allows the waveguide structure along the *Z* axis of the crystal to be formed. Figure 5*a* shows the result of probing of the structure formed with displacement of the exposure spot along the *Z* axis of the crystal. The exposure step size was 60 μm.

The possibility of forming exposure areas along the *Z* axis of the crystal allows waveguide structures of complex topology to be induced in photorefractive layers. The typical example of the structure with complex topology is shown in Fig. 5*b*. Light beam exposure of channel optical waveguides was used in [15] for modulation of the parameters of rectilinear waveguide elements obtained by diffusion of titanium into the $LiNbO_3$ substrate. The results obtained by the authors demonstrated that the point-by-point exposure can be used to form a more complex topology defined by the form of the light spot trajectory on the sample surface in the photorefractive layers of waveguide systems.

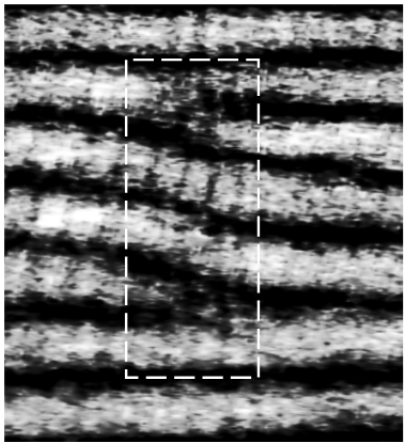

Fig. 6. Light image at the exit from the Jamin interferometer with the examined sample inserted in one of the interferometer shoulders.

The change of the refractive index Δn induced by point-by-point exposure of waveguide structures in the surface crystal layer was quantitatively estimated using a Jamin interferometer. Interferograms were recorded by a CCD camera. An example of such interferogram is shown in Fig. 6. From the interferogram it can be seen that in the induced area of the crystal marked in Fig. 6, the phase shift of the interference band $\Delta\varphi$ is observed compared with the sample without laser-induced changes of the refractive index. The phase shift of the interference bands was $\Delta\varphi = 1.1\pi$. The change in the refractive index Δn was quantitatively estimated from the formula [16]

$$\Delta = (n_1 - n_2)\, d = \Delta n d, \tag{1}$$

where n_1 is the refractive index of the crystal, n_2 is the refractive index of the crystal changed upon exposure to laser radiation, d is the thickness of the doped layer, and Δ is the difference between the beam paths. Calculations demonstrated that the refractive index in the exposure area changed by $\Delta n = 1 \cdot 10^{-3}$.

CONCLUSIONS

Thus, the possibilities of forming the induced channel waveguide structures with spatial modulation of their parameters have been experimentally demonstrated. For point-like exposure, the opportunity arises to influence the longitudinal homogeneity of the waveguide channels and hence to form waveguide channels along the polar axis of the $LiNbO_3$ crystal. This allows one to form in the doped surface crystal layer channel waveguides and their systems with complex topology determined by the light spot trajectory on the sample surface. Such structures admit repeated optical reconfiguration and can be used in optical devices of photonics.

This work was performed within the framework of the Design Part of the State Assignment of the Ministry of Science and Higher Education of the Russian Federation for 2017–2019 (Project on the Application No. 3.1110.2017/PCH), the Design Part of the State Assignment for 2017–2019 (Project No. 3.8898.2017/8.9), and was supported in part by the Russian Foundation for Basic Research (Grant No. 316-29-14046-ofi_m)

REFERENCES

1. J. E. Toney, Lithium Niobate Photonics, Artech House, Boston; London (2015).
2. E. Krätzig and O. Schirmer, in: Photorefractive Materials and Their Applications I, No. 61, P. Günter and J. P. Huignard, eds., Springer, Berlin; Heidelberg (1988), pp. 131–166.

3. M. P. Petrov, S. I. Stepanov, and A. V. Khomenko, Photorefractive Crystals in Coherent Optics [in Russian], Nauka, Saint Petersburg (1992).
4. V. M. Shandarov, Russ. Phys. J., **58**, No. 10, 1378–1386 (2015).
5. D. Kip, Appl. Phys. B, **67**, 131–150 (1998).
6. Y. S. Kivshar and G. P. Agrawal, Optical Solitons: from Fibers to Photonic Crystals, Academic Press (2003).
7. M. Morin, G. Duree, G. Salamo, and M. Segev, Opt. Lett., **20**, No. 20, 2066–2068 (1995).
8. G. C. Valley, M. Segev, B. Crosignani, *et al*., Phys. Rev. A, **50**, R4457 (1994).
9. V. Shandarov, D. Kip, M. Wesner, and J. Hukriede, J. Opt., A, **2**, 500–503 (2000).
10. F. Chen, Laser Phot. Rev., **6**, No. 5, 622–640 (2012).
11. J. Kushibiki, T. Kobayashi, H. Ishiji, and C. K. Jen, J. Appl. Phys., **85**, No. 11, 7863–7868 (1999).
12. S. A. Davydov, P. A. Trenikhin, V. M. Shandarov, *et al*., Phys. Wave Phen., **18**, No. 1, 1–6 (2010).
13. A. D. Bezpaly, A. O. Verkhoturov and V. M. Shandarov, Ferroelectrics, **515**, No. 1, 34–43 (2017).
14. A. D. Bezpaly, A. O. Verkhoturov, and V. M. Shandarov, Proc. SPIE, **10603**, 10603-1–10603-6 (2017).
15. A. Kanshu, C. E. Rüter, D. Kip, and V. M. Shandarov, Appl. Phys. B, **95**, No. 3, 537–543 (2009).
16. M. Born and E. Volf, Principles of Optics [Russian translation], Nauka, Moscow (1973).